JOURNAL OF MATERIALS SCIENCE 20 (1985) 3535–3544

Microstructure refinement with forced convection in aluminium and superalloys

G. S. REDDY*, J. A. SEKHAR
Defence Metallurgical Research Laboratory, PO Kanchanbagh, Hyderabad 500258, India

The cooling and average local solidification times were determined for slow solidification of Al–4.4 wt% Cu alloy under natural convection and under electromagnetically forced axisymmetric rotation during liquid cooling and solidification in graphite moulds. Cooling rates were measured with *in situ* thermocouples. The conditions needed to stabilize the radial temperature gradient with rotation were established. The microstructure size decreased with increasing rotation, as did the local solidification times. The average grain and dendrite size without imposed rotation is coarser near the mould wall compared with the centre of the casting. This trend is reversed with imposed rotation. Rotation also led to a smaller spread of grain and dendrite size at any chosen height of the casting. These results are discussed in relation to existing theories, and several reasons for an improved heat transfer coefficient with rotation are presented. Forced convective solidification was then carried out for various shapes of integral investment cast Nimonic-90† alloy solidifying under modified conditions that prevented columnar grain formation. Similar results to those recorded for the aluminium case were obtained and are presented here. The major conclusion is that observations indicating a reduction of microstructure spacing during forced convection should also consider improved heat extraction at the mould–metal interface.

List of symbols

Gr = Grashof number = $\dfrac{g\beta\Delta T Z^3 \varrho^3}{\eta^3}$

g_r = acceleration in radial direction
g_θ = acceleration in θ direction
g_Z = acceleration in Z direction (gravity)
h = heat transfer coefficient
k_l = thermal conductivity of liquid

Nu_Z = Nusselt number = $\dfrac{hZ}{k_l}$

Pr = Prandtl number = $\dfrac{\eta}{\varrho\alpha}$

Ra = Rayleigh number $Gr\,Pr$

R = radius of mould

Re_r = Reynolds number = $\dfrac{\varrho V_0 R}{\eta}$

T = temperature
ΔT = temperature difference in radial direction

Ta = Taylor number = $\dfrac{\varrho^2 4H^4 W^2}{\eta^2}$

V = velocity
W = r.p.m.
α = thermal diffusivity
β = coefficient of volume expansion
η = viscosity
ϱ = density

*Mr G. S. Reddy is also a post graduate student registered at the Banaras Hindu University, Varanasi, India.
† The nominal composition of Nimonic-90 is (Ni–16 Co–20 Cr–3 Ti–1 Al–0.06 C).

0022–2461/85 $03.00 + .12

1. Introduction

Fine and narrowly distributed grain structures exhibit high strength at low temperatures, reduced anisotropy and enhanced high cycle fatigue properties. Obtaining fine grain structures during solidification is possible by several techniques such as (a) rapid application of pressure [1]; (b) supercooling the alloy to increase the nucleation rate [2, 3] (homogeneous nucleation rate is an exponential function of supercooling); (c) addition of grain refiners to increase the number of heterogeneous nucleation sites with a further check on grain coarsening by the additon of growth inhibitors [4]; (d) ultrasonic vibration or supercooling to promote cavitation and high pressures required for suddenly increased probability of nucleation [5, 6]; (e) rapid cooling followed by compacting of fine powders including consolidating and crystallizing metallic glass [7–9]; and (f) grain multiplication by remelting or fracturing growing dendrites and dispersing the pieces to act as growth centres for the rest of the solidification process [10, 12]. Grain multiplication is known to be possible by ultrasonic vibration, by fluid flow as natural and forced convection, by a recalescence process, or by dendrite coarsening [10–13]. A narrow distribution of grain size should be available by providing for a similar thermal and compositional environment during the grain formation history at all locations in the casting.

Unless the grain refiners are of a similar composition to the cast metal itself [14], strict control of chemistry and the use of brittle ceramic shell moulds during net shape casting mean that only the supercooling and grain multiplication techniques are viable for castings such as superalloy-grade integral cast turbines. The former is more restrictive in practice. The study of grain and dendrite refinement for a slowly cooled aluminium alloy and investment cast nickel-based superalloy under axisymmetric forced convective conditions forms the topic of this paper.

The effect of fluid flow on grain multiplication has been studied by several authors. Tiller *et al.* [10] have concluded that fluid motion during solidification leads to an increased probability of grain multiplication and refinement by either the segmentation of dendrites and the misalignment of the separated segments or by the buckling and misorientation of a dendritic array. They showed that even a velocity of $0.25\,\mathrm{m\,sec^{-1}}$ of fluid past an array of dendrites could cause bending stresses of a magnitude greater than 1 MPa. Stress magnitudes of this order were sufficient to cause deformation of dendrites and the local adiabatic heat generated by this process could cause melting or recrystallization. Similarly movement of hot liquid to the roots of secondary arms can cause melting and separation [12]. In turbulent flow conditions local eddies along the dendrites may also lead to fatigue-type conditions and separation from the parent grain may occur [10]. In the limit, vigorous agitation leads to "stir cast microstructure" with the elimination of the dendritic network and is associated with a beneficial drop in strength of the partially formed semi-solid body [15]. In a recent important development Vogel [16] and Lee *et al.* [17] have shown evidence for plastic bending, recrystallization and clustering in turbulently agitated aluminium alloys. Previously, experimental evidence for dendrite remelting and distribution by heat pulses arriving at the root of the dendrites had been presented [12].

It seems evident that the coupled nature of the fluid flow and heat flow is important to predict grain size. The relationship between structure and imposed experimental conditions to cause or suppress fluid motion has previously been studied. Flow of a fluid in front of a growing array of dendrites has been shown to change the direction and towards the upstream direction [17–19]. Cole and Bolling [20] have shown that Coriolis fields in rotating sections may prevent natural convection and aid a columnar growth structure. They further showed that an acceleration/deceleration fluid flow condition at the solid–liquid interface could lead to detachment of crystals at the interface and promote equiaxed grains. More recently Johnston and Parr [21] showed that an increase in the acceleration level produced dendrite fragmenting. Similarly the effects of natural convection in aiding or suppressing columnar growth have recently been studied again [22]. Convection also plays a major role in liquid penetration of the intercellular regions during solidification, thereby causing macrosegregation [23–25]. Vigorous convection may also disturb the solidification pattern even during eutectic solidification

[26–28]. In the present study we aim to characterize in detail the effect of various degrees of high fluid velocity on grain formation and cooling rate for an axisymmetric cylindrical-type mould rotation. Fonseca de Arruda *et al.* [29] have shown the limitations of the depth of grain refinement on rotating the mould to force liquid rotation by transmitting shear stresses from the mould wall to the fluid. The present study involves a travelling electromagnetic field-type induction motor winding to induce body forces in the liquid, to causing it to rotate concentrically within the mould. Fully stable flow conditions, as predicted [30] by the square of the momentum increasing outwards from the centre, may become available by this technique at least as long as solidification does not occur. Similar techniques have been used previously [31, 32] to alter the solidification pattern during crystal growth. In more recent investigations [33–35] unstable electromagnetically induced fluid oscillations have been shown to produce grain refinement in aluminium alloys.

2. Experimental procedure

Liquid Al–4.4% Cu–0.12% Si alloy was stirred in a cylindrical graphite mould employing an electromagnetic induction stirrer. The induction stirrer was simply an induction motor without the shaft assembly. The shaft assembly is replaced by the mould metal configuration. The alloy was originally charged into a fireclay crucible and melted in an electric resistance furnace. A schematic diagram of the configuration during stirring is shown in Fig. 1. Liquid metal was stirred at different speeds of rotation by varying the input voltage of the apparatus. The speed of rotation (r.p.m.) of the alloy was measured using a stroboscope for different input voltages and the results are plotted in Fig. 2. This curve is valid only for the aluminium alloy considered and changes with material being agitated.

The graphite mould, of internal diameter 58 mm, 170 mm long with a side wall thickness of 6 mm and bottom wall thickness of 16 mm, was preheated to a temperature of 550° C in an electric resistance furnace prior to loading into the stirring apparatus. Three chromel/alumel thermocouples with twin-bore recrystallized alumina sheaths were inserted into the mould at different locations: centre, edge and wall as shown in Fig. 1. All the thermocouples were projected to an equal height of 25 mm from the bottom of the mould. The initial liquid height was maintained at approximately 50 mm from the bottom of the mould. A fourth thermocouple was embedded in the bottom wall of the crucible. The mould was placed on an insulating asbestos pad initially at room temperature. Temperatures were recorded by a quick-

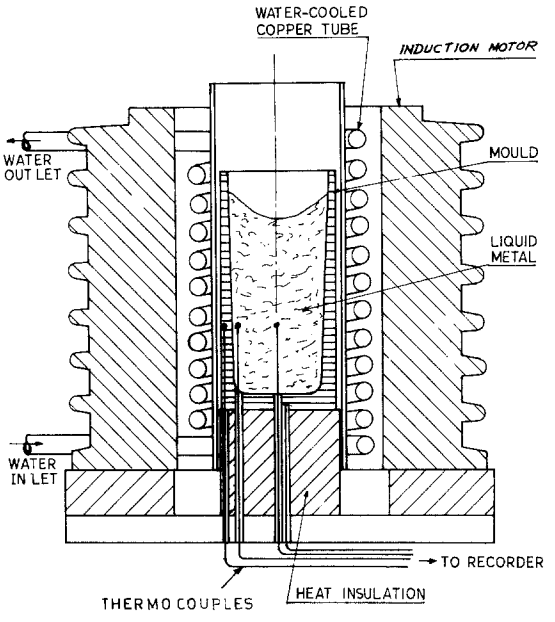

Figure 1 Schematic representation of the graphite mould and casting kept inside the induction stirrer. Also shown are the locations of the four thermocouples. The water-cooled copper tube does not make contact with the mould and is kept to protect the motor windings.

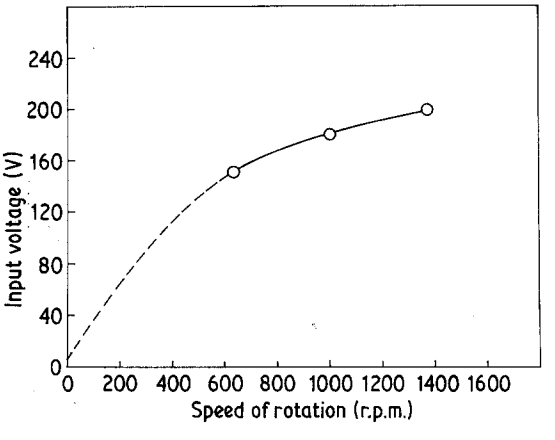

Figure 2 The measured r.p.m. (measured by a stroboscope) for the imposed voltage on each phase of the induction motor. The broken line is the extrapolation to lower voltages.

response four-pen recorder of 0.2 sec full-scale response. Temperature measurement without the liquid in the graphite crucible but with the stirrer on indicated that there was no heating in the mould on account of any induced currents.

The cooling curves were recorded for the alloy with *in situ* thermocouples. The local solidification time was estimated from these cooling curves by assuming that the liquidus and eutectic temperatures were 926 K and wherever eutectic arrest occurred (normally ~812 K). The casting was cut longitudinally into two halves and further sectioned horizontally. The micro- and macrostructures of the longitudinal and transverse surfaces were examined within 25 mm from the tip of the centre thermocouple junction. Keller's reagent was used for microstructures and 15% H_2SO_4 + 5% HF solution was used for macrostructure examination. Dendrite arm spacing was measured at the centre and edge of the sample by a mean linear intercept method from photomicrographs for each of the samples. As will be evident from the photomicrographs presented in the following section, no distinction could generally be made between primary and secondary arms. Similarly the macroetchant solution given above was used for grain size measurement. In all cases the average grain size so revealed was the same within statistical error as the dendrite arm aim for this slowly solidified alloy composition. Above five photomicrographs at × 50 were recorded from each cut section of the casting and, on average, intercepts from more than 10 randomly placed lines were recorded from each photograph.

Nickel-based superalloys were cast in several shapes of zircon investment material mould, with and without electromagnetic stirring. "Nimonic-90" alloy was air melted in an induction melting furnace in a magnesia-lined crucible and poured at a temperature of 1550° ± 20° C into the preheated moulds (1100° C) placed within the stirrer motor. In these experiments the alloy was agitated with interrupted stirring with a cycle corresponding to 3 sec on/1 sec off until solidification was complete. The cast discs were cut longitudinally into two halves for microstructure examination. Dendrite arm spacings were measured by the mean linear intercept method as mentioned above.

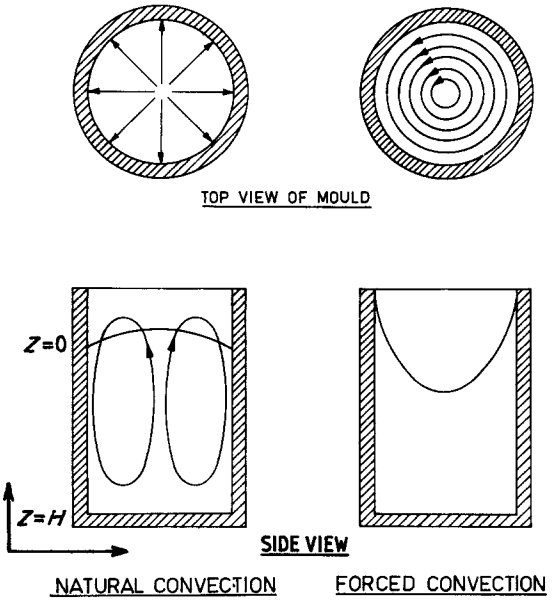

Figure 3 Schematic representation of fluid motion for natural and forced convection.

3. Results and discussion

3.1. Heat flow

Analysis of heat flow during solidification is essential for correlation of the spacings of the final cast microstructure with processing conditions. Casting into the mould involved pouring the liquid of a predetermined superheat into the preheated mould kept on the cold asbestos pad. The combined influence of the heat removed by the walls and bottom of the mould aided or hampered by convection in the presence of solidification heat liberation will determine the thermal history at all locations. The parameter of interest is h, the heat transfer coefficient. For the two cases considered (Fig. 3), the situation should classically be described as:

$$Nu = f(Pr, Gr, \ldots) \text{ natural convection} \quad (1)$$

$$Nu = f(Pr, Re, \ldots) \text{ forced convection}$$

where Nu is the Nusselt number, Pr is the Prandlet number and Gr is the Grashof number. Normally these equations imply that the heat transfer is enhanced by increasing the temperature gradient and hence fluid velocity for natural convection, and increasing fluid velocity in the direction of heat transfer in forced convection. The equations classically only account for the rate of heat being supplied to the mould–metal interface and do not take into account any

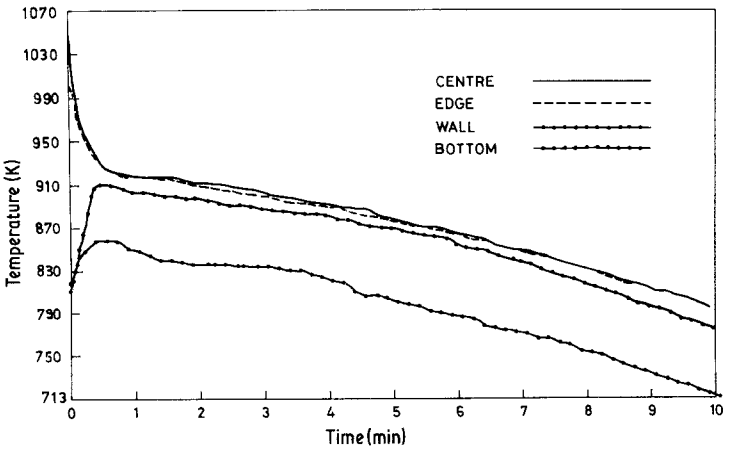

Figure 4 Cooling curve for the Al–4.4 wt % Cu alloy during no agitation. The level of radial temperature measurement was at $Z = 0.5H$. The bottom thermocouple was kept at the $r = 0$ position.

physical changes in contact at the interface itself. As discussed below, evidence from our experiments suggests that these physical changes may also be important.

The heat transfer coefficient should vary along the height of the crucible, i.e. along the axis; extending the analysis of Cole [36], the position of the average heat transfer coefficient (h) during natural convection, i.e. where the average and local heat transfer coefficients become equal, should be located at (see Appendix for the calculations)

$$Z = 0.66H \tag{2}$$

The measurement of the heat transfer coefficient at this location should be adequate to describe the average heat flow conditions during liquid cooling. In practice, however, during forced convective conditions the real value of h is a dynamic quantity varying with meniscus height and the average value of h is no longer ideally at Z given by Equation 2. As this paper involves a comparison of grain structure for the two possibilities of Fig. 3, a fixed value of $Z = 0.5H$ was chosen as the level of measurement, where H refers to the poured height (50 mm).

The radial temperatures and bottom wall temperature for the case of natural convection (no forced agitation) are shown in Fig. 4. Solidification ($T = 926$ K) begins after 25 sec and there are no radial temperature gradients in the liquid cooling stage or after significant solidification, i.e. the casting mass is always radially isothermal, indicating (i) a low value of wall heat transfer coefficient and/or (ii) the natural convection evening out the gradient. In contrast, for the case of forced convection (Fig. 5) at 630 r.p.m. (150 V), a radial temperature difference of 34 K is observed when the edge temperature was 953 K, and the temperature gradient persists even after solidification is complete. In the absence of forced convection, a zero radial temperature difference in the liquid is a reasonable indication of zero axial temperature difference unless as established by pure conductive heat removal from the bottom of the mould. This happens in cases such as shown in Fig. 4. Rotation at lower speeds could not prevent the radial temperature difference created by the Coriolis field but progressively established the

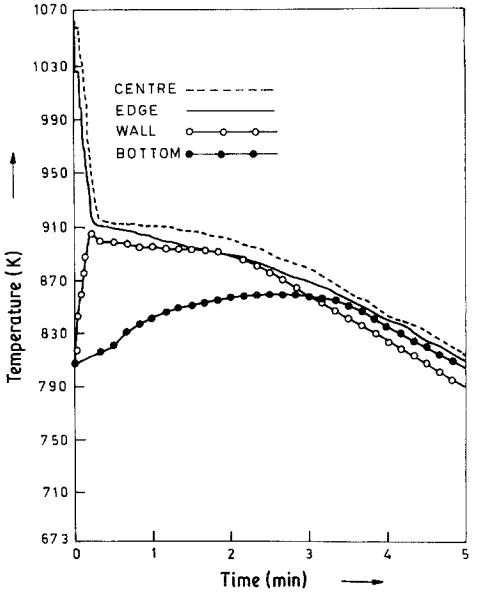

Figure 5 Cooling curve for the Al–4.4 wt % Cu alloy during forced agitation at 630 r.p.m. The radial temperature measurement was at $Z = 0.5H$. The bottom thermocouple was kept at the $r = 0$ position.

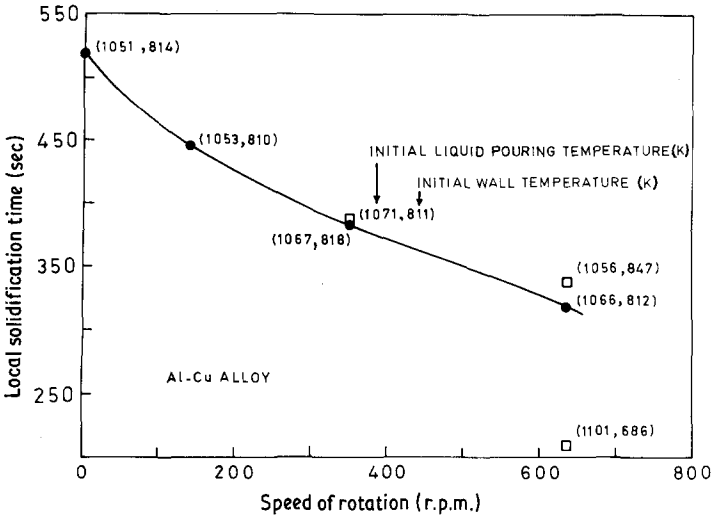

Figure 6 Effect of rotation on the local solidification times at the centre of the casting. These times were calculated from temperature measurements of the type shown in Figs. 5 and 6.

temperature gradient after the mass stopped rotating, i.e. on forming a high fraction mass solid bridge. These are indications that forced convection led to an increased Nusselt number during liquid cooling and also that the effects of this increased heat transfer in the liquid state actually promoted a high heat transfer coefficient during subsequent solidification and solid cooling.

The measured local solidification time (t_f) at the centre of the casting mass with increasing amounts of rotation is plotted in Fig. 6. For all experiments performed during this investigation the local solidification time at the centre and close to the edge wall were identical within ± 3 sec. A decrease of > 200 sec in the local solidification time is seen by increasing the rotation from 0 to 630 r.p.m. The Fig. 6 also shows that even at 350 and 630 r.p.m. the t_f is sensitive to both the initial pouring temperature and the initial mould temperature. In the regime of measurements with a fixed geometry of the casting, t_f can empirically now be given as:

$$10^{-3} t_f^2 = k(269.36 - 0.23W)_{C_1, C_2} \quad (3)$$

where the constants k, C_1, C_2, are the units, material and geometric constants of the casting and mould material and W is the imposed rotation (r.p.m.). A family of such curves for various C_1, C_2, etc., would be a useful engineering compilation.

The additional force in a convecting liquid, i.e. the Coriolis force, is known to prevent natural convection and impede convective heat transfer [36]. This further leads to a radial temperature difference such as observed in Fig. 6. Natural convection [31] (which evens out the radial temperature gradients) is absent when

$$Ra(\text{crit}) < Ta^2(\text{crit}) \quad (4)$$

where Ra(crit) and Ta(crit) are the critical Rayleigh and Taylor numbers demarcating the convection and convection-free regions. This relationship or a modified form of it including radial accelerations generated by the electromagnetic field are obviously satisfied at 630 r.p.m.

In the present study the use of forced convection actually led to an increased liquid cooling rate and solidification rate even in the presence of the radial temperature gradient as compared to the case of no gradient. This may be attributed to the fact that forced convection actually provided for a better pressure contact with the mould and therefore led to an increased heat transfer coefficient. This improved pressure contact should be possible by (i) the radial pressure gradient and (ii) an improved smoother contact if the rotation led to erosion of asperities on the inner mould wall. This increased heat transfer coefficient leads to a better cooling rate being observed even after the solid network formed is large enough to impede rotation. Such an increase in heat transfer coefficient with pressure has been reported previously during squeeze casting [37] where, however, the range of pressures studied was uniform and much larger than those expected during rotation.

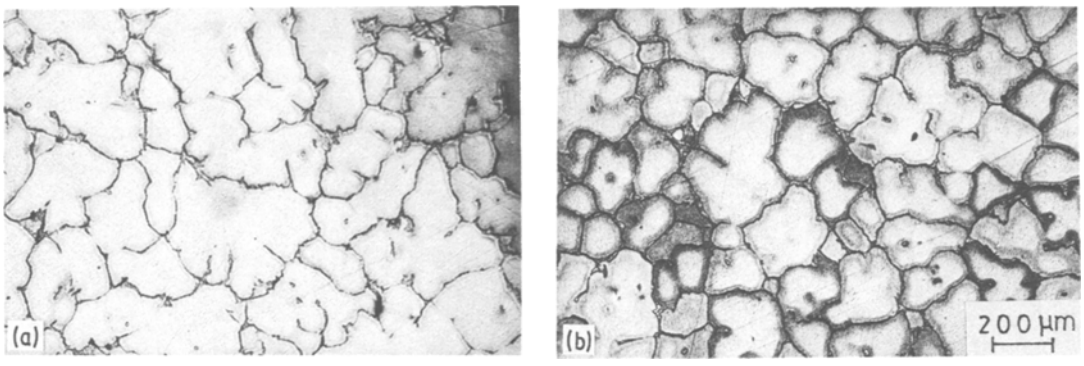

Figure 7 Photomicrographs of Al–4.4 wt % Cu alloy solidified with no imposed rotation: (a) from a region close to the wall of the casting; (b) from a region at the centre of the casting.

3.2. Dendrite and grain size

The typical equiaxed dendritic grains seen at the edge and centre of the casting for the two cases of no rotation and rotation are shown in Figs 7 and 8 respectively. For this particular alloy (unlike the superalloy discussed below), the grain and dendrite size are the same. Figs. 7a and b show the grain structure obtained for the case of natural convection (no agitation). The grain size at the centre is smaller than at the edge on account of solidification debris accumulation during natural convection. This trend reverses itself when rotation is imposed, as shown in Figs. 8a and b for the case of rotation at 630 r.p.m. Compositional analysis along the radial direction for all the casting indicated no severe macrosegregation. The maximum deviation in composition was ± 0.2 wt % Cu and the excess tended to occur somewhere midway between the edge and centre. In Fig. 9 the measured variation of the average dendrite arm spacing (DAS) (i.e. the average equiaxed dendrite size with rotation) is shown. The dramatic drop in DAS with rotation and the reversal of the centre/edge dendrite size with rotation is evident from this figure. The effect of rotation is to narrow the value of the standard deviation with increasing amount of rotation. The data are statistically significant, as described in the experimental section above.

A simple relationship has been seen to be valid between the average cooling rate during solidification and the secondary dendrite arm spacing [38]. In Fig. 10 the full line (Bower *et al.* [39]) gives the accepted relationship for Al–4.5 wt % Cu alloys. Also shown in the figure are the average dendrite sizes obtained in this work (with the Al–4.4 wt % Cu–0.1 % Si alloy from Figs. 6 and 9). These points do not fall on the full line and also as indicated in Fig. 9 the scatter around these mean points is somewhat large but decreases with rotation, which reduces the local solidification times. This is a significant observation, i.e. local processing must also be important in determining the DAS. In fact somewhat contradictory analyses by Johnston *et al.* [21]

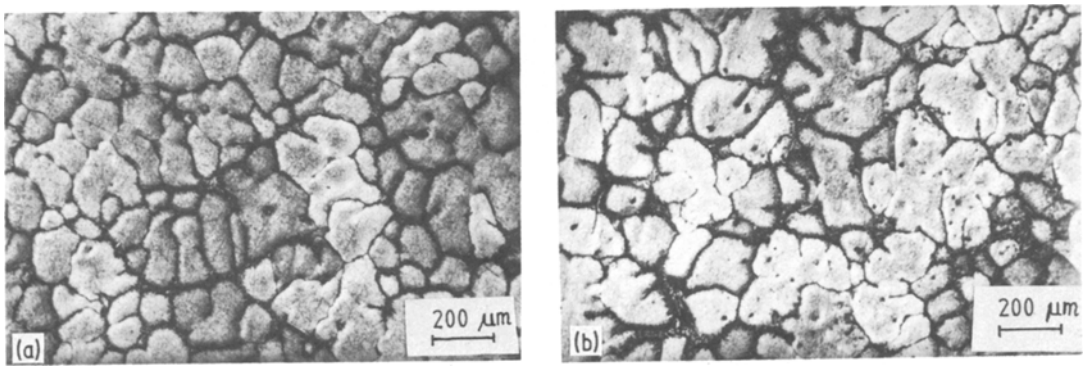

Figure 8 Photomicrographs of Al–4.4 wt % Cu alloy solidified with an imposed rotation of 630 r.p.m.: (a) from a region close to the wall of the casting; (b) from a region at the centre of the casting.

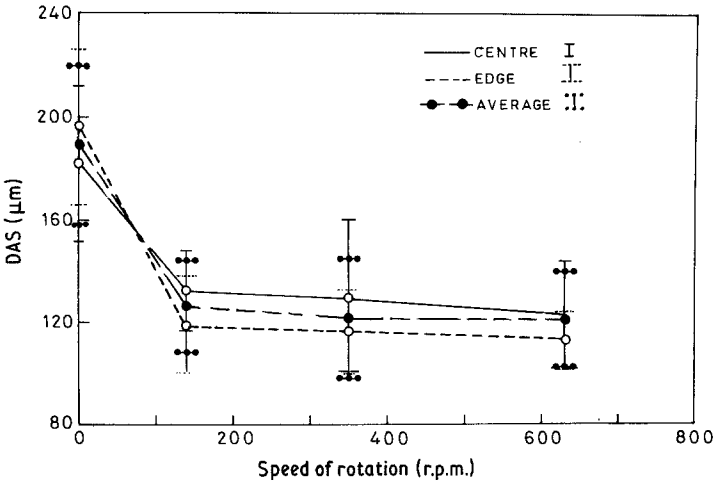

Figure 9 Effect of rotation on the dendrite arm spacing (DAS) of the Al–4.4 wt % Cu alloy. The bars represent the standard deviation from the respective mean values.

and Doherty and co-workers [40, 41] have previously specifically focused on the fact the fluid flow influences the coarsening of dendrites.

The increase in the number of grains/dendrites in the absence of a stable positive radial temperature gradient also seems to indicate that multiplication occurs by detachment caused by dendrite fracture (most probably by high-energy boundary formation [40]) and by remelting. Increasing rotation and then heat extraction aids this by causing a greater local gradient and thus more solid detachable protrusions, in all likelihood thus explaining the origin of the greater number of distinct solid identities. The effect is, however, possibly more complex on account of the combined influence of the local solidification time determining the tortuosity, and the velocity of the fluid determining the difference in solute mixing behaviour during each experiment.

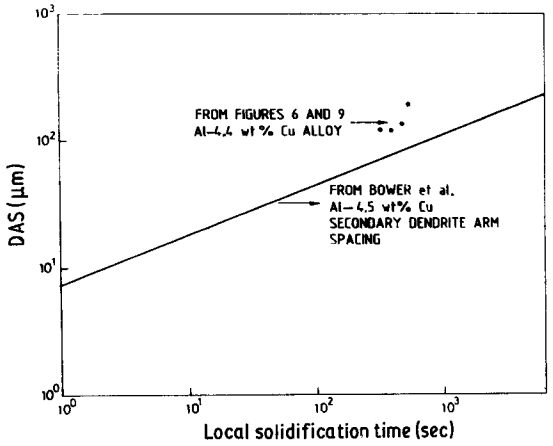

Figure 10 Plot showing the log–log relationship between secondary dendrite arm spacing and local solidification time for an Al–4.5 wt % Cu alloy (from Bower *et al.* [39]). Also shown by the black dots are the average values obtained during this work from Figs. 6 and 9. The measurements in this work (i.e. of equiaxed dendrites) relate to primary dendrite arm spacings.

3.3. Investment cast superalloy

Fluid rotation was applied to the shapes shown in Fig. 11. The alloy used was Nimonic-90†. In addition to continuous rotation, the stirring was interrupted for 1 sec after every 3 sec of continuous rotation. This was done to prevent the natural tendency of superalloys to define a well aligned columnar structure and is somewhat similar to the oscillatory stirring employed by other researchers [33, 42]. In Fig. 11 we find that dendrites size consistently reduces with rotation even though rotation was not continuous. (Note that, for any fixed geometry, increasing voltage corresponds to faster rotation.) There is also an effect on the grain size but the effect is not as prominent.

4. Conclusion

The effect of axisymmetric rotation of an aluminium alloy at high velocity (caused by an electromagnetic driving force) in a graphite mould is (a) to stabilize the radial temperature gradient, (b) to refine the grain size, (c) to refine the dendrite arm spacing, (d) to reduce the scatter in the grain and dendrite sizes at any chosen height of the casting and (e) to cause reversal of the central edge grain sizes.

The dendrite arm size is reduced on account of rotation leading to improved heat transfer rates, because of better contact of the casting with the

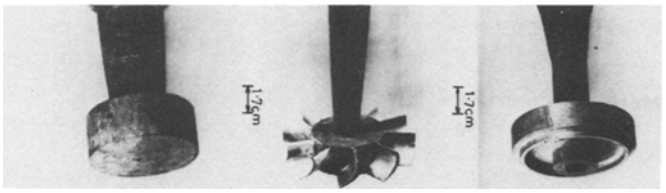

Figure 11 Grain and dendrite spacing of three shapes of investment cast Nimonic-90. The accompanying table shows effect of voltage on grain size (GS) and dendrite arm spacing (DAS); the standard deviations are given in parentheses.

Volts	0	0	180
GS(mm)	4.46	3.04	2.48
	(0.96)	(0.79)	(0.45)
DAS(μm)	165	164	105
	(16.09)	(43.3)	(13.8)
Volts	–	225	200
GS(mm)	–	2.12	2.5
	–	(0.3)	(0.35)
DAS(μm)	–	136.9	92.7
		(13.7)	(18.9)

mould. This was revealed by measuring the average local cooling and solidification times in the mould and the casting. Rotation at 630 r.p.m. leads to the local solidification time being reduced by > 200 sec and the average equiaxed dendrite size being reduced by $> 70\ \mu$m when compared to the case of no rotation. The increased rate of cooling with imposed rotation is evident during the liquid cooling stage and also during solid cooling after the solidification is complete. Observations on the local solidification times and the dendrite arm size indicate that relating the two would require some knowledge of how local fluid influences the coarsening.

Similar results are obtained for a nickel-based superalloy solidifying in various investment shell moulds. These results indicate that observations showing a reduction in microstructurs spacing with imposed fluid flow should take into account any improved heat transfer characteristics at the mould–metal interface.

Appendix: Calculations for location of average Nusselt number during natural convection [36]

We have

$$\frac{h_Z Z}{k_l} = 0.508 \frac{(Pr)^{1/4}}{Pr + 0.952} (Gr_Z\ Pr)^{1/4} \quad \text{(A1)}$$

and

$$\frac{h_{ave} H}{k_l} = 0.67 \frac{(Pr)^{1/4}}{Pr + 0.952} (Gr\ Pr)^{1/4} \quad \text{(A2)}$$

Hence

$$h_Z = h_{ave} \quad \text{at } Z = 0.66H \quad \text{(A3)}$$

i.e. assuming a constant ΔT in the calculation of Gr and Gr_Z.

Acknowledgement

The authors thank Dr P. Rama Rao, Director, DMRL, for encouragement and permission to publish this work.

References

1. J. A. SEKHAR, M. MOHAN, C. DIVAKAR and A. K. SINGH, *Scripta Metall.* **18** (1984) 1327.
2. D. TURNBULL, *Solid State Phys.* **3** (1956) 225.
3. G. J. ABBACHIAN and M. C. FLEMMINGS, *Metall. Trans.* **14A** (1983) 1147–1157.
4. See, for example, A. HELLAWELL "Solidification and Casting of Metals" (The Metals Society, 1979).
5. For review, see J. CAMPBELL, *Int. Met. Rev.* **26** (2) (1981) 71.
6. G. HORVAY, Proceedings of the 4th National Congress of Applied Mechanics (AISME, 1962) p. 3115.
7. P. K. DOMALAVAGE, N. J. GRANT and YIGAL GEFEN, *Metall. Trans.* **14A** (1983) 1599.
8. R. RAY, "Rapidly Solidified Amorphous and Crystalline Alloys", edited by B. H. Kear, B. C. Gissen and M. Cohen (North-Holland, New York, 1982) p. 435.
9. J. A. SEKHAR and S. H. RISBUD, *J. Non-Cryst. Solids* **47** (1982) 363.
10. W. A. TILLER and S. O. O'HARA, "The Solidification of Metals" (Iron and Steel Institute, London, 1967) p. 27.
11. J. L. WALKER, "Physical Chemistry of Process Metallurgy", Part I (Interscience, New York, 1961).
12. K. A. JACKSON, J. D. HUNT, D. R. UHLMANN and T. P. STEWARD, III, *Trans. Met. Soc. AIME* **236** (1966) 149.

13. M. C. FLEMMINGS, "Solidification Processing" (McGraw-Hill, New York, 1974).
14. J. CAMPBELL and P. D. CATOM, "The Solidification and Casting of Metals" (The Metals Society, 1979) p. 208.
15. P. A. JOLY and R. MEHRABIAN, *J. Mater. Sci.* **11** (1976) 1393.
16. A. VOGEL, *Met. Sci.* **12** (1978) 576.
17. H. I. LEE, R. D. DOHERTY, E. A. FEEST and J. M. TITCHMARSH, "Solidification Technology in the Foundry and Cast House" (The Metals Society, London, 1983) p. 143.
18. B. CHALMER, "Principles of Solidification" (Wiley, 1964).
19. K. MURAKAMI, T. FUJIYAMA, A. KOIKE and T. OKAMOTO, *Acta Metall.* **31** (9) (1983) 1425.
20. G. S. COLE and G. F. BOLLING, "Solidification Technology", edited by J. J. Burke, M. C. Flemmings and A. L. Gorum (Brook Hill Publ. Co., Mass., 1974) p. 189.
21. M. H. JOHNSTON and R. A. PARR, *Metall. Trans.* **13B** (1982) 35.
22. H. FREDRIKSSON, "Materials Processing in Reduced Gravity Environments of Space", edited by G. E. Rindone (Elsevier, 1982) p. 619.
23. S. D. RIDDER, F. C. REYES, S. CHAKRAVORTY, R. MEHRABIAN, J. D. NAUMAN, J. H. CHEN and H. J. KLEIN, *Metall. Trans.* **9B** (1978) 415.
24. R. MEHRABIAN, M. KEANE and M. C. FLEMMINGS, *ibid.* **1** (1970) 1209.
25. J. P. GABATHULER and F. WEINBERG, *ibid.* **14B** (1983) 733.
26. J. M. QUENISSET and R. NASLAIN, *J. Cryst. Growth* **54** (1981) 465.
27. J. JUNZE, K. F. KOBAYASHI and P. H. SHINGU, *Metall. Trans.* **15A** (1984) 307.
28. N. APAYADIN, *J. Mater. Sci. Lett.* **1** (1982) 39.
29. A. C. FONESCA DE ARRUDA and M. PRATES DE CAMPOS FELHO, "Solidification Technology in the Foundry and Cast House" (The Metals Society, London, 1983).
30. G. I. TAYLOR, *Phil. Trans. R. Soc.* **A223** (1923) 289.
31. H. K. MOFATT, *J. Fluid Mech.* **22** (1965) 521.
32. W. C. JOHNSTON and W. A. TILLER, *Trans. TMS–AIME* **221** (1961) 331.
33. F. A. CROSSLEY, *The Iron Age* **8** (1960) 102.
34. A. NISHIMURA, Y. KAWANO and K. FUJITA, *Aluminium* **60** (1984) E512.
35. A. NISHIMURA and Y. KAWANO, *J. Jp. Inst. Light Met.* **25** (1973) 193.
36. G. S. COLE, "Solidification" (ASM, Metals Park, Ohio, 1971) p. 211.
37. J. A. SEKHAR, G. J. ABBASCHIAN and R. MEHRABIAN, *Mater. Sci. Eng.* **40** (1979) 105.
38. R. MEHRABIAN, "Rapid Solidification Processing – Principles and Technologies" (Claitors Publ., Baton Rouge, USA, 1978).
39. T. F. BOWER, H. D. BRODY and M. C. FLEMMINGS, *Trans. AIME* **236** (1966) 624.
40. A. VOGEL, R. D. DOHERTY and B. CANTOR, Proceedings of Conference on Solidification and Casting of Metals, Sheffield, July 1977 (Metals Society, London, 1979) p. 518.
41. R. D. DOHERTY, HO-INLEE and E. A. FEEST, *Mater. Sci. Eng.* **65** (1) (1984) 181.
42. G. S. COLE and G. F. BOLLING, *Trans. TMS–AIME* **233** (1965) 1568.

Received 2 April
and accepted 2 November 1984